Journal of Machine Construction and Maintenance
PROBLEMY EKSPLOATACJI
QUARTERLY ISSN 1232-9312 3/2017 (106)
p. 21–30

**Mateusz SAKÓW, Krzysztof MARCHELEK, Arkadiusz PARUS, Karol MIĄDLICKI**
Department of Mechanical Engineering and Mechatronics, West Pomeranian University of Technology, Szczecin,
mateusz.sakow@zut.edu.pl; krzysztof.marchelek@ps.pl; arkadiusz.parus@zut.edu.pl; karol.miadlicki@zut.edu.pl

# CONTROL SCHEME WITHOUT FORCE SENSORS FOR LOAD SENSING IN TELEMANIPULATION SYSTEMS WITH FORCE-FEEDBACK

**Key words:** Teleoperation, force-feedback, inverse modelling, robotics, remote control.

**Abstract:** The paper presents a novel approach to the control design of bilateral teleoperation systems with force-feedback dedicated only for weight sensing. The problem statement, analysis of related papers up to date, and the scope of the study are presented. The new design of a control unit for a master-slave system with force-feedback was based on an inverse model. The model was applied to subtract a value of force in the force-feedback communication channel that the system might generate during free-motion. A substantial part of the paper is focused on the development of a mathematical model for the investigated control scheme. The paper presents the modelling procedure of the experimental setup and the model used in the study. Two experiments are described to demonstrate the control unit of the master-slave system with force-feedback. The paper contains conclusions regarding to the control and the experimental setup.

## Bezsensorowy schemat sterowania dedykowany do wyczuwania ładunku w systemach telemanipulacyjnych z siłowym sprzężeniem zwrotnym

**Słowa kluczowe:** zdalna operacja, siłowe sprzężenie zwrotne, odwrotne modelowanie, robotyka, zdalne sterowanie.

**Streszczenie:** W artykule przedstawiono nowe podejście do projektowania sterowania dwustronnych systemów obustronnego działania ze sprzężeniem siłowym zwrotnym, przeznaczonym wyłącznie do wykrywania obciążenia. W artykule został zaprezentowany opis problemu, analiza dotychczasowych osiągnięć badawczych oraz zakres badania. Nowy projekt jednostki sterującej dla systemu Master-Slave ze sprzężeniem siłowym zwrotnym oparty został na modelu odwrotnym. Model został użyty do odejmowania wartości siły w kanale komunikacyjnym sprzężenia zwrotnego, który jest generowany przez system podczas ruchu swobodnego. Znaczna część pracy koncentruje się na opracowaniu modelu matematycznego obejmującego zjawiska występujące w badanym schemacie kontroli. W pracy przedstawiono wnioski dotyczące systemu kontroli oraz omówiono procedurę modelowania konfiguracji eksperymentalnej oraz model zastosowany w układzie sterowania. Opisane są dwa eksperymenty, aby zademonstrować jednostkę sterującą systemu master-slave ze sprzężeniem siłowym zwrotnym. W pracy przedstawiono również wnioski dotyczące wyników eksperymentalnych.

## Introduction

The researchers' attempts to ensure the safe operation of various machines have led to the development of master-slave control systems with force-feedback. The applications of master-slave systems are widespread, including performing tasks in environments hostile to man, contaminated sites, in the depths of oceans and seas, radioactive interiors of nuclear power plants, and even other applications like medical rehabilitation. Most of master-slave systems are unilateral [11, 12, 17, 23, 25, 30, 31], i.e. a device that is being controlled, which is the slave subsystem, should behave exactly as the device that controls it, which is the master subsystem. However, as research continued, it was noticed that the operator that interacts with the master subsystem/manipulator should be able to feel the haptic effect of the environment on the slave subsystem side. The problem posed significant challenges in its practical application due to large distances and the inevitable time delay [1–5, 9, 10, 13, 14, 16–18, 22–27, 33, 39, 40]. This specific branch of robotics faces many challenges that have been conducted by researchers all over the world for many years. The main problem concerns the communication channel, and it is a transport time delay that is inhibiting their communication. The problem is particularly pronounced

while sending information over large distances. Another challenge is the stability of such systems, given known or unknown delays in the communication channel.

So far, the sensor-less bilateral teleoperation domain of science mostly belongs to piezoelectric crystals. Piezoelectric crystals can work at the same time as actuator, body, and a force sensor, especially, when developing devices from a large group of single crystals. Yusuke Ishikiriyama and T. Morita in 2010, published a paper about the self-sensing control method of piezoelectric actuators that compensate for the hysteresis characteristics by using the linear relationship between the permittivity change and the piezoelectric displacement [7]. Also in 2010, Micky Rakotondrabe focused his research on the dynamic self-sensing of the motion of piezoelectric actuators [20]. The proposed measurement technique was subsequently used for a closed-loop control. Aiming to obtain a self-sensing scheme that estimates the transient and steady-state modes of the displacement, the author extended a previous static self-sensing scheme by adding a dynamic part. Again in 2011, Micky Rakotondrabe developed a new micro-gripper dedicated to micromanipulation and micro-assembly tasks [19]. Based on a new actuator, called a thermo-piezoelectric actuator, the micro-gripper provided high-range and high-positioning resolution. Finally, Micky Rakotondrabe continued his studies and in 2015, and he presented his work about a self-sensing technique using an actuator as a sensor at the same time [24, 32]. This was possible for most actuators with a physically reversible principle, such as piezoelectric materials.

So far, the main presented control schemes for bilateral teleoperation systems with force-feedback have some defects. These defects required the use a large number of sensors mediating between the environment and the bodies of the slave manipulator, especially in rotary joints. A situation in which the environment affects one degree of freedom in accordance with that degree of freedom is relatively simple by using a single sensor. However, where the design of the manipulator depends on many degrees of freedom, and moves in the three-dimensional space, the use of a single or multiple sensors could be considered as expensive, or not adequate for the proper operation of such a system.

Large sensor-less and self-sensing appliances are rare, even in scientific literature. There are only couple of papers that address the problem of inverse modelling used in self-sensing control units of bilateral teleoperators. This work and papers [6, 15, 22, 23, 25, 28, 29, 36, 37] address this problem. The first paper [37] presents a method for the impedance control of a pneumatic linear actuator for tasks involving contact interaction. The presented method takes advantage of the natural compliance of pneumatic actuators. The central notion of the method is that, that by departing from a stiff actuation system, low-bandwidth acceleration measurements can be used in lieu of high-bandwidth force measurements. The second paper [32] presents teleoperated minimally invasive surgery systems measurement and display of a sense of force to the operator. In this paper, a master-slave system for laparoscopic surgery is proposed, which can provide force-feedback to the surgeon without using force sensors. Pneumatic cylinders were used as the actuator of the manipulators to achieve this. Both papers are based on the same control methodology, which is the impedance control. In [37], control methodology contained an inner loop to control the pressure on two sides of a pneumatic cylinder, while an outer loop enforces an impedance relationship between external forces and motion and commands desired pressures to the inner loop. The inner loop enforces the natural compliance of the pneumatic actuator by controlling both the sum and difference of the pressures on both sides of the pneumatic actuator. In [32], a bilateral dynamic control system was designed using a neural network for the acquisition of the inverse dynamics. The obtained inverse dynamics was used as a feed-forward controller and to estimate the external force from the differential pressure of the cylinders.

In our research, we designed a control scheme for a master-slave system with force-feedback. The difference between sensor methods is thus far that, in the case of the proposed control scheme, there are no sensors mediating between the manipulator body and the environment, relative to papers [6, 15, 28, 29, 36, 37]. The same thing can be noticed in self-sensing and piezo-ceramic micromanipulators used for micromanipulation an in impedance control methods [7, 8, 19–21, 34, 35, 38]. The only sensors used in whole system are position encoders and pressure sensors. The whole manipulator body is considered as a perfectly rigid body. In this paper, the operator needs to feel the manipulator load, but also a haptic effect of a contact is required. Contact between the object of the environment was realized in the way that the system will push back the operator, in the situation with an unmovable object.

Additionally, the paper presents a pneumatic manipulator that is an introduction to the work on the crane car, which is much bigger then devices in the presented literature. In this project, the operator needed to feel the crane load, but the feeling of a haptic contact was also required. The introduction to work on much bigger devices means the consideration of disadvantages like long hydraulic pipes, which are also included in the presented test-stand. The problem of high friction values and many other problems which will occur during further work have to be overcome during preliminary tests.

Also in this paper, part of impedance control was used. This part is an inverse model of the manipulator structure corresponding to the manipulator operation without any environmental impact on the slave subsystem. Based on this fact, it is possible to obtain relatively accurate information about the environmental impact on the specific DOF of the slave manipulator. This important feature eliminates the need of using a sensor (susceptible

component) between the body of the manipulator and the environment, or between the actuator and the manipulator body.

An important feature of this approach on the design of the control system is that the value of the impact of the environment is transmitted to a specific master manipulator degree of freedom, as a response from the equivalent DOF in the slave manipulator, but without using geometrical relationships resulting from the construction of the manipulator. The difference between impedance control [32, 37] in this system is relatively simple. The control unit is not controlling the pressure inside an actuator chamber. Measured pressure is only being subtracted by the estimated pressure, and the estimated pressure is calculated by the inverse model of slave subsystem.

## 1. Self-sensing control scheme for teleoperation with perfectly rigid bodies

The presented sensor-less control scheme for bilateral teleoperation consists of two subsystems - the master subsystem and the slave subsystem. Both subsystems, the Master (a) and the Slave (b), are considered as simple rigid objects described by their inertia, and they are presented in Fig. 1.

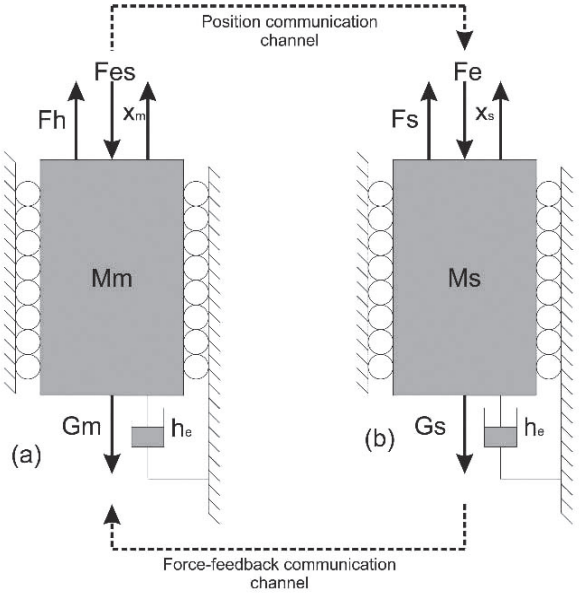


**Fig. 1. Graphical presentation of models: master subsystem (a), the slave subsystem (b)**

These manipulator bodies move in an environment described by the dissipative element $h_e$. The damper represents, for example, a simplified centre of air and any other type of motion resistance. The bodies of the manipulators move without friction between them, and the global coordinate system. Master subsystem acts as a motion scanner, which sends information about its own position $x_m$ to the slave manipulator.

Master subsystem motion depends on three forces applied to the body of Master manipulator. The first is the gravity, described as $G_m = M_m g$, where $g$ is the acceleration of gravity and $M_m$ is the mass of the body. The second force is the force applied by the operator $F_h$, to the body of the Master manipulator. The last force applied to the body of Master manipulator is $F_{es}$, which is transferred in communication channel from slave subsystem. For theoretical analysis transmittance of master subsystem actuator, the resisting operators' motion is not considered. Furthermore, in the case of theoretical analysis, the inverse model represents an idealized object, and there are no noises considered in the control scheme.

During analysis, the slave subsystem is a duplicate of the master subsystem under conditions of kinematics, dimensions, and mass. This subsystem also moves in the same environment as the master subsystem. The slave manipulator is described by its mass – $M_s$, gravity force $G_s$, position – $x_s$, control force $F_s$ (theoretically including Slave actuator) that is generated by the actuator, and the environmental impact by force $F_e$. The transfer function $B_i$ that describes the dynamics of both manipulators can be presented as Equation (1):

$$B_i = \frac{1}{\left(M_i s + h_e\right) s} \tag{1}$$

where $i$ – index, index m for master subsystem, index $s$ for slave subsystem, $s$ – Laplace operator, $M_i$ – mass.

## 2. Telemanipulation control schemes

Standard telemanipulation system using force sensors can be represented as a block diagram as in Fig. 2.

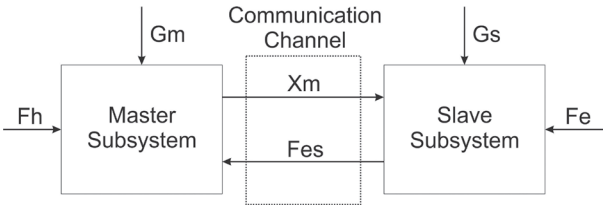


**Fig. 2. Block diagram of standard sensor method**

In Fig. 2, the system senses the environmental force impact by the force sensor and sends the value of force back to the Master manipulator in the communication channel $F_{es}$.

In the presented work, the system do not measure environmental force impact, but it estimates its value based on the control signals of the slave controller and the current Slave manipulator position. The modified structure of the telemanipulation system is presented in Fig. 3.

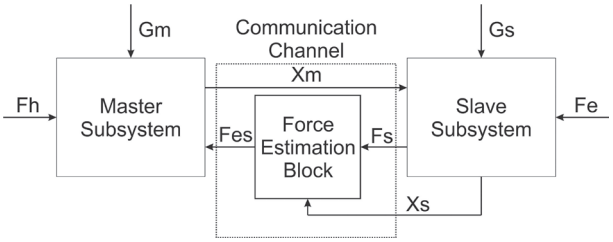


**Fig. 3. Block diagram of the presented method with the force-feedback estimation block**

In Fig. 3, the system has an additional block. The estimation block calculates the force of environmental impact based on the force value computed by the model of the slave subsystem. The force-feedback estimation block subtracts the measured control signal of the drive from what is estimated by the model in free motion. This measured force could be a hydraulic pressure, a voltage or as presented in this paper, a hydraulic valve current. The modified system is described in detail in Fig. 4.

The primary problem of methods, where force sensors and rotary joints are being used, is that the control unit needs a large number of force sensors placed on the manipulator arm. This feature is crucial to deliver the correct value of environmental torque impact in each rotary joint. In this work, the method computes the value of environmental force impact on the slave manipulator to the operator, which is measured in the drive track in each joint of the Slave manipulator independently. The presented system requires as many sensors of current, voltage, or pressure, as there are dimensions of freedom included in the Slave manipulator structure. Rotary or linear joints do not benefit from the presented method of the estimation of environmental forces on each joint in the force-feedback communication channel. As a result, the system, based on the presented method of estimation, the force-feedback channel will send to the Master manipulator a zero value of force during free motion of Slave manipulator.

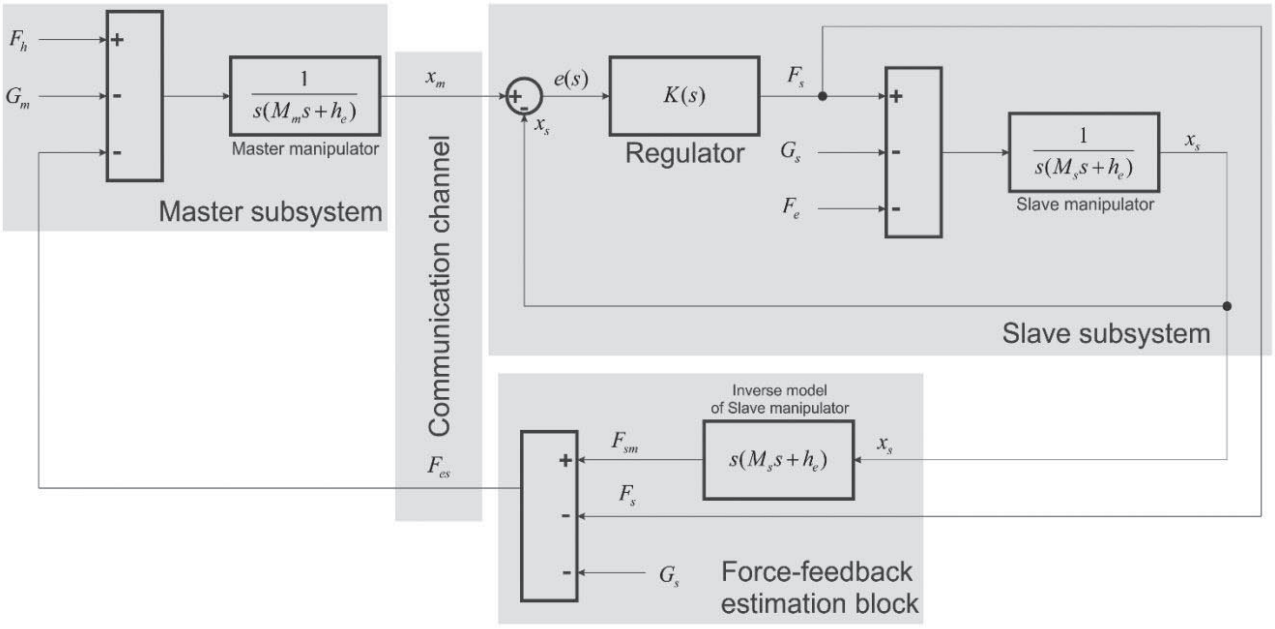


**Fig. 4. Block diagram of the system in details that was used for the analysis**

## 3. Theoretical system analysis

First characteristic transmittance, which describes Slave side of the telemanipulation system, is a transmittance without the impact of gravity force and environmental force on the Slave manipulator – Fig. 4. The gravity force and the environmental force are described by Equation (2):

$$G_s = 0;\ F_e = 0 \tag{2}$$

To investigate the effectiveness of the presented method, it is required to find the slave subsystem closed-loop and the inverse model transmittances by reducing the slave subsystem transmittance (Fig. 4) to a simple transfer function. The first transfer function describes the relation of two signals $x_m$, which is the position of Master, send to Slave, and the $x_s$ which is the position of Slave. The transmittance $x_s/x_m$ is presented as Equation (3):

$$\frac{x_s(s)}{x_m(s)} = \frac{K(s)}{(M_s s+h_e)s+K(s)} \tag{3}$$

Equation (3) describes the closed-loop system of the Slave manipulator, including the transfer function of the position controller K(s). The controller transfer function is unknown for the transmittance analysis, because it is possible to use many structures of controllers, e.g., simple proportional P, PI, or even PID. Different controller structures would not change the result of the presented method.

In a continuation of transmittance analysis, the slave subsystem closed-loop transfer function is determined as (3). The Second transmittance, including the inverse model of force-feedback estimation block and the closed-loop of slave subsystem, is defined by a ratio of the estimated value of the force generated by the drive during the free motion of the Slave manipulator – named $F_{sm}$ and the Master position – $x_m$, and transmittance $F_{sm}/x_m$ is presented by Equation (4):

$$\frac{F_{sm}(s)}{x_m(s)} = \frac{K(s)(M_s s + h_e)s}{(M_s s + h_e)s + K(s)} \tag{4}$$

Equation (4) describes one of two characteristic transfer functions, which is the function that is responsible for reducing the value of force in a force-feedback communication channel. Force in the communication channel of the manipulator system using rotary joints without additional force-feedback estimation block sends to the operator and master subsystem a value of force used to achieve the desired configuration of the Slave manipulator. This force will depend on actual position of each joint and its acceleration, including the inertia of individual bodies. This feature appears only during free-motion conditions.

The next step requires finding the transmittance of closed-loop Slave system, which senses the control signal $F_s$ from the controller's block K(s) output. Theoretically, this signal is just the control force applied to the body of the Slave manipulator. In practice, the control signal on the Slave side could be a voltage, a current, or a pneumatic pressure as presented in the third part of this paper. To find this transfer function, it is required to find a solution of two equations presented as follows:

$$\begin{cases} F_s = K(s)e(s) \\ x_s = \dfrac{F_s}{(M_s s + h_e)s} \end{cases} \tag{5}$$

where e(s) is a slave subsystem position error, described as $e(s) = x_m(s) - x_s(s)$. Looking for a solution of the equations (5) by a ratio of $F_s(s)/x_m(s)$, we obtain Equation (6):

$$\frac{F_s(s)}{x_m(s)} = \frac{K(s)(M_s s + h_e)s}{(M_s s + h_e)s + K(s)} \tag{6}$$

exactly the same as transmittance (4). This means that the slave subsystem , during free-motion in a remote environment, calculates zero value in the force--feedback communication channel. This is confirmed by the transmittance difference, which is represented as the force-feedback estimation block in Fig. 4 and by Equation (7):

$$F_{es} = \frac{F_s(s)}{x_m(s)} - \frac{F_{sm}(s)}{x_m(s)} = 0 \tag{7}$$

For the operator of a system, which uses the presented method, this situation is comfortable, but requires a very accurate inverse model of slave subsystem. It is important to show that the slave subsystem, which is under influence of the environmental force, sends to the operator exactly the force of the environmental impact. Of course, in this case, the theoretical analysis is based on the ideal system presented in Fig. 4.

In the second part of transmittance analysis (4) and (6), external forces are taken into account. These forces were omitted during the first analysis to proof that system in a free-motion situation calculates the correct value of the estimated force in the Force--feedback communication channel. Two new equations are obtained (8) and (9), which describes the slave subsystem in Fig. 4, including external forces:

$$\frac{F_{sm}(s) - G_s}{x_m(s)} = \frac{K(s)(M_s s + h_e)s}{(M_s s + h_e)s + K(s)} \tag{8}$$

$$\frac{F_s(s) - G_s - F_e}{x_m(s)} = \frac{K(s)(M_s s + h_e)s}{(M_s s + h_e)s + K(s)} \tag{9}$$

Subtracting Equations (8) and (9), we obtain Equation (10):

$$F_s(s) - G_s - F_e - F_{sm}(s) + G_s = 0 \tag{10}$$

After simplifying Equation (10), Equation (11) was obtained:

$$F_s(s) - F_{sm}(s) = F_e \tag{11}$$

where the difference $F_s(s) - F_{sm}(s)$ according to the control scheme of Fig. 4, corresponds to the signal of force-feedback communication channel $F_{es}$, presented as Equation (12):

$$F_{es} = F_e \tag{12}$$

## 4. The experimental test stand

Mechanical features of a slave and a master subsystem are completely identical. The exoskeleton master subsystem was attached to the operator's elbow. The subsystem slave was mounted on a strong and heavy table. Thus, it was not necessary to do the calculations of pressure in the feedback resulting from differences in the mass and dimensions of the master and the slave. The mass of the human limb was considered as negligible. The experimental setup is presented in Fig. 5.

Figure 5 presents the manipulator arm with its drive system, which was taken into account in the mathematical model of a pressure in chambers. There is a stationary base plate (1), which is fixed to the table. The bending actuator (5) and its extension bend the manipulator arm. The straightening actuator (2) and its extension straighten the manipulator arm (3). The characteristic manipulator arm is the movable part of the slave subsystem (3). The arm rotates at the articulated wrist, where a measuring encoder was mounted.

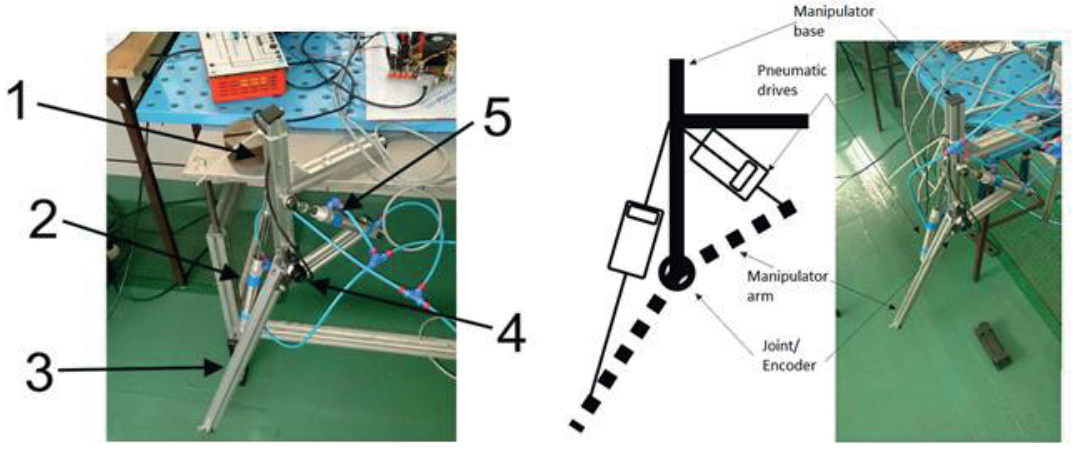


**Fig. 5. Experimental test-stand**

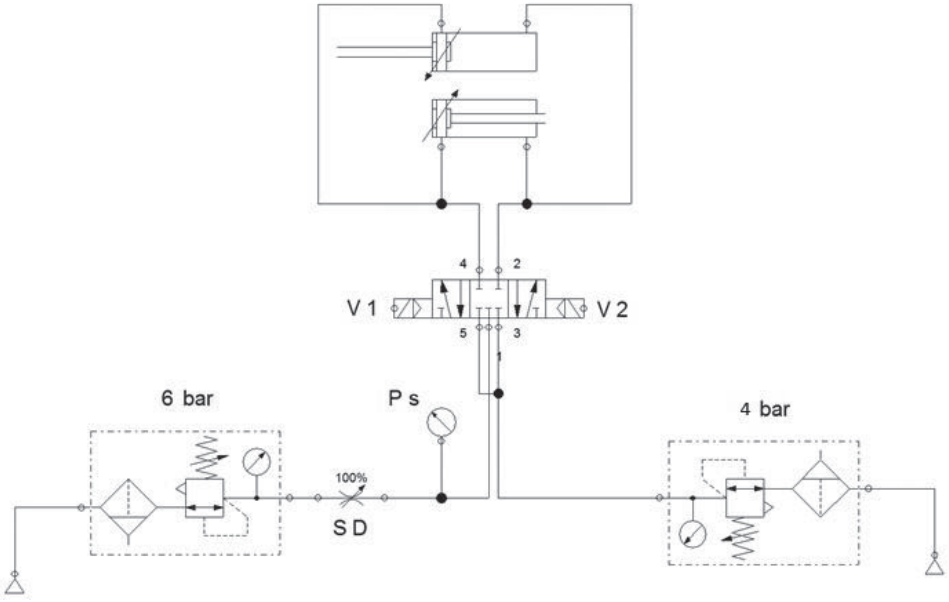


**Fig. 6. Pneumatic scheme of Slave manipulator**

Mounting pneumatic drives in the presented way was not accidental. Using two drives affects the symmetry of the piston areas which, as it turned out, considerably improved the position tracking ability of the entire subsystem slave. Most of signals in the system are analogue signals, e.g., the pressure measurement, and discrete for the encoders and valves. Encoders that were used to build the test-stand had a number of pulses equal to 500 per revolution. The pressure gauge used to measure pressure in the system had a maximum measurement value of 10 bar, proportionally sensing the pressure as 1 to 10 V.

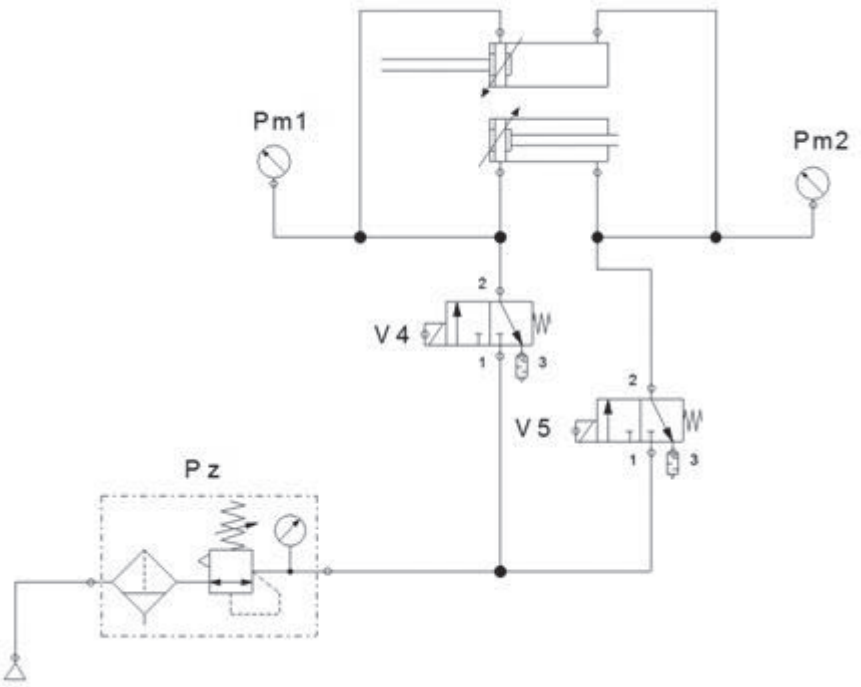


**Fig. 7. Pneumatic scheme of Master manipulator**

In the slave subsystem, as shown in Fig. 6, there are three pneumatic control signals $V_1$, $V_2$, and SD. The $V_1$ signal is the left coil voltage signal of 5/3 switching valve, $V_2$ is the right coil voltage signal of the same switching valve, and the SD signal is analogue and controls the degree of throttle opening – the variable orifice. The pressure sensor $P_s$ is placed between the 5/3 Valve and the variable orifice. As it turned out during tests, it is possible to estimate pressure in both piston chambers using a single pressure sensor, with a respect to a pneumatic scheme in the Fig. 6. In the case of the master subsystem, it was easy to use a pressure control valve $P_z$ that controls the air pressure on the basis of the set value from force-feedback communication channel. Then, the pressure will only reach the destined piston chambers using on/off valves, $V_4$ and $V_5$ (Fig. 7), and the additional pressure sensors, $Pm_1$ and $Pm_2$, were not needed in the control scheme.

## 5. Inverse modelling of the test stand

Based on Equations (1) to (12), it is possible to build a model of a slave subsystem that describes the dynamics of the system.

During the modelling procedure, it was obvious that there was a model of a geometrical structure of the slave subsystem required, which was actually a nonlinear manipulator arm model. Based on the manipulator arm, a geometrical and dynamic model of the slave and master subsystem was built, as shown in Fig. 8. The geometrical model of a rotating arm was dependent on the dimensions of actuators. The dimensions of each actuator cause movement of the entire manipulator arm. To build a model that will behave exactly like the one in Fig. 5 requires the use of geometrical relationships among actuator, base, and the rotational arm of the manipulator, as shown in Fig 8.

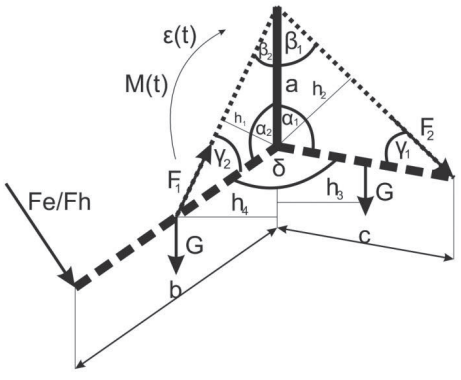


**Fig. 8. Geometrical relationship of manipulator arm**

The model presented in Fig. 8 describes the estimated pressure in free motion at the time domain by Equation (13):

$$P_{est}(t)=\frac{G_2 esin\left(\beta_2(t)\right)-G_1\frac{d}{2}\sin\left(\beta_1(t)\right)-\frac{1}{3}\left(m_1c^2+4m_2b^2\right)\varepsilon(t)}{\left(A_2 bcos\left(\frac{\pi}{2}-\gamma_2\right)-A_1 bsin\left(\gamma_1\right)\right)} \tag{13}$$

where $A_1$ and $A_2$ are the areas of pistons – first and second actuator, ε(t) is the angular acceleration of the manipulator arm, $G_1$ and $G_2$ are the gravity forces applied to the body of manipulator. Rest variables are angles and radiuses used to derive Equation (13) – see Fig. 8.

As it turned out during tests, a simple geometric and mechanical model was not enough to properly estimate pressure inside the piston chamber. This model was incorporated into the structure of nonlinear autoregressive model with exogenous input – NARX. The nonlinear part of model NARX was based on a binary tree. This model has estimated the pressure relatively well, relative to simple Equation (13).

## 6. Experiment

After the identification was carried out, the model of the slave subsystem tests were conducted to verify the operation of the whole system. The aim of the first measurement was to check how the system would behave, given no interaction with the environment. The only interaction of the environment, which occurs for the nonlinear manipulator arm, is gravity and resistance to motion, and in this particular case, the friction and resistance of air surrounding the manipulator. However, even these component data were modelled within the structure of the NARX model. Owing to this, such a data can be considered as negligible, when conducting certain runs by the slave subsystem of the manipulator, because they exert the same influence both on the real object and on the model. Diagrams of the first experiment are presented in Fig. 9.

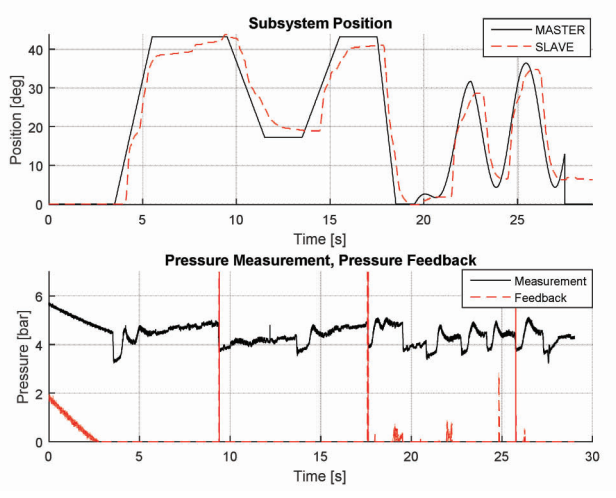


**Fig. 9. Master-slave system test-stand; first measurement during free motion operation**

The aim of the second experiment was to check if the system would show the maximum pressure at the moment when it encounters an object it would not be able to move. The results of the experiment are shown in Fig. 10.

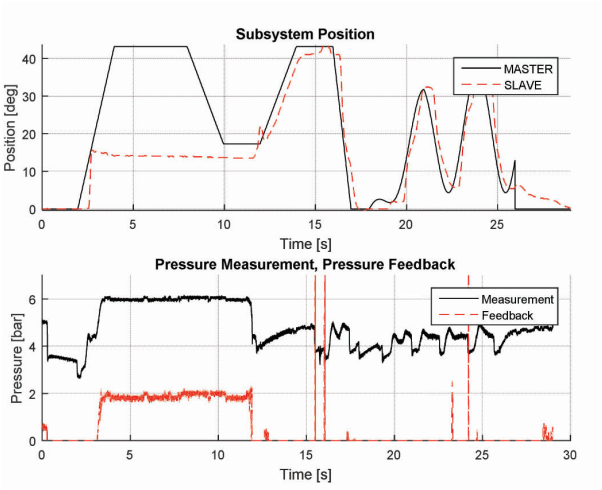


**Fig. 10. Master-slave system test-stand; second measurement during contact operation**

The contact phase can be seen in the runs presented in Fig. 10 between 3 to 12 seconds. The control system precisely mapped the maximum pressure of 2 bars. The maximum pressure of 2 bars in force feedback is the effective pressure, resulting from using the control method that relies on pressure changes in the system. The maximum pressure in the system is 6 bars. However, it is counteracted by the pressure of 4 bars, and the whole system stiffens. The value of 2 bars means that the system was able to transmit adequate information to the feedback with a relatively large time delay of 0.5 s. It can even be seen in Fig. 10. This is due to the compressibility of the medium in the system, and it is not the fault of the control system, whose clocking frequency was set a 10 kHz.

## Conclusion

The paper addresses the problem of self-sensing, sensor-less bilateral teleoperation. The control unit was based on a NARX model of subsystem Slave. The tests were conducted on a short distance of one meter, so that any delay in the communication channel was negligible. But the width of a pipe delivering air pressure between actuator chamber and pressure sensor affected a delay of around 0.5 s. The additional difficulty of the main task of the study was the fact that the rotating robotic arm was driven by two linear pneumatic actuators. Two linear pneumatic actuators were mounted in the presented way to overcome the difference in a cylinder surface. This difference caused serious modelling problems. The actuators were also mounted so that their characteristics would be strongly nonlinear, i.e. the radial length of the actuator retraction axis to the rotation axis of the arm

would not be constant but would be dependent on the configuration of the robot arm at a given time – a feature of car cranes.

An additional challenge was posed by the pneumatic system itself. One disadvantage of pneumatic systems may be the fact that they are quite difficult to control, when it comes to position tracking. This can be due to high air compressibility, which translates into low stiffness of the mechanical structure. For position tracking, a simple PID controller was used that cooperated with a controllable orifice. The controller was tuned during system operation. The simple PID controller was used, because this paper was not focused on ability of position tracking by the system, but on a proof that the system is able to estimate the values of force-feedback without a force sensor and impedance control method.

## Acknowledgements

The work was carried out as part of PBS3/A6/28/2015. „The use of augmented reality, interactive voice systems, and operator interface to control a crane," that was financed by NCBiR.

## References

1. Ben-Dov D., Salcudean S.E., A force-controlled pneumatic actuator for use in teleoperation masters, Robotics and Automation, 1993. Proceedings., 1993 IEEE International Conference on, 1993, pp. 938–943 vol. 933.
2. Ferrell W.R., Delayed Force Feedback, Human Factors: The Journal of the Human Factors and Ergonomics Society, 8 (1966) 449–455.
3. Guerriero B., Book W., Haptic Feedback Applied to Pneumatic Walking, ASME 2008 Dynamic Systems and Control Conference, American Society of Mechanical Engineers, 2008, pp. 591–597.
4. Hannaford B., Stability and performance tradeoffs in bi-lateral telemanipulation, Robotics and Automation, 1989. Proceedings., 1989 IEEE International Conference on, 1989, pp. 1764–1767 vol. 1763.
5. Hastrudi-Zaad K., Salcudean S.E., On the use of local force feedback for transparent teleoperation, Robotics and Automation, 1999. Proceedings. 1999 IEEE International Conference on, 1999, pp. 1863––1869 vol. 1863.
6. Hogan N., Impedance Control: An Approach to Manipulation: Part II – Implementation, Journal of Dynamic Systems, Measurement, and Control, 107 (1985) 8–16.
7. Ishikiriyama Y., Morita T., Improvement of self-sensing piezoelectric actuator control using permittivity change detection, Journal of Advanced Mechanical Design, Systems, and Manufacturing, 4 (2010) 143–149.
8. Khadraoui S., Rakotondrabe M., Lutz P., Interval Modeling and Robust Control of Piezoelectric Microactuators, Control Systems Technology, IEEE Transactions on, 20 (2012) 486–494.
9. Kim W.S., Developments of new force reflecting control schemes and an application to a teleoperation training simulator, Robotics and Automation, 1992. Proceedings., 1992 IEEE International Conference on, 1992, pp. 1412–1419 vol. 1412.
10. Kim W.S., Hannaford B., Fejczy A.K., Force-reflection and shared compliant control in operating telemanipulators with time delay, Robotics and Automation, IEEE Transactions on, 8 (1992) 176–185.
11. Miądlicki K., Pajor M., Overview of user interfaces used in load lifting devices, International Journal of Scientific & Engineering Research, 6 (2015) 1215–1220.
12. Miądlicki K., Pajor M., Real-time gesture control of a CNC machine tool with the use Microsoft Kinect sensor, International Journal of Scientific & Engineering Research, 6 (2015) 538–543.
13. Najdovski Z., Nahavandi S., Fukuda T., Design, Development, and Evaluation of a Pinch– Grasp Haptic Interface, Mechatronics, IEEE/ASME Transactions on, 19 (2014) 45–54.
14. Nguyen T., Leavitt J., Jabbari F., Bobrow J.E., Accurate Sliding-Mode Control of Pneumatic Systems Using Low-Cost Solenoid Valves, Mechatronics, IEEE/ASME Transactions on, 12 (2007) 216–219.
15. Ningbo Y., Hollnagel C., Blickenstorfer A., Kollias S.S., Riener R., Comparison of MRI-Compatible Mechatronic Systems With Hydrodynamic and Pneumatic Actuation, Mechatronics, IEEE/ASME Transactions on, 13 (2008) 268–277.
16. Noritsugu T., Pulse-width modulated feedback force control of a pneumatically powered robot hand, International Symposium of Fluid Control and Measurement, Tokyo, 1985, pp. 47–52.
17. Pajor M., Miądlicki K., Saków M., KINECT SENSOR IMPLEMENTATION IN FANUC ROBOT MANIPULATION, Archives of mechanical technology and automation, 34 (2014) 35–44.
18. Polushin I.G., Takhmar A., Patel R.V., Projection-Based Force-Reflection Algorithms With Frequency Separation for Bilateral Teleoperation, Mechatronics, IEEE/ASME Transactions on, 20 (2015) 143–154.
19. Rakotondrabe M., Ivan I.A., Development and Force/Position Control of a New Hybrid Thermo-Piezoelectric MicroGripper Dedicated to Micromanipulation Tasks, Automation Science and Engineering, IEEE Transactions on, 8 (2011) 824–834.

20. Rakotondrabe M., Ivan I.A., Khadraoui S., Clevy C., Lutz P., Chaillet N., Dynamic displacement self-sensing and robust control of cantilever piezoelectric actuators dedicated for microassembly, Advanced Intelligent Mechatronics (AIM), 2010 IEEE/ASME International Conference on, 2010, pp. 557–562.
21. Rakotondrabe M., Ivan I.A., Khadraoui S., Lutz P., Chaillet N., Simultaneous Displacement/Force Self-Sensing in Piezoelectric Actuators and Applications to Robust Control, Mechatronics, IEEE/ASME Transactions on, 20 (2015) 519–531.
22. Saków M., Miądlicki K., Parus A., Self-sensing teleoperation system based on 1-dof pneumatic manipulator, Journal of Automation, Mobile Robotics and Intelligent Systems, 11 (2017) 64–76.
23. Saków M., Pajor M., Parus A., Estymacja siły oddziaływania środowiska na układ zdalnie sterowany ze sprzężeniem siłowym zwrotnym o kinematyce kończyny górnej, MODELOWANIE INZYNIERSKIE, 58 (2016) 113–122.
24. Saków M., Pajor M., Parus A., Układ sterowania samowyznaczający siły oddziaływania środowiska na manipulator wykonawczy w czasie pracy systemu telemanipulacyjnego, Projektowanie Mechatroniczne – Zagadnienia Wybrane, Katedra Robotyki i Mechatroniki, Akademia Górniczo-Hutnicza w Krakowie, 2016, pp. 139–150.
25. Saków M., Parus A., Sensorless control scheme for teleoperation with force-feedback, based on a hydraulic servo-mechanism, theory and experiment, Measurement Automation Monitoring, 62 (2016) 417–425.
26. Saków M., Parus A., Miądlicki K., Predykcyjna metoda wyznaczania siły w siłowym sprzężeniu zwrotnym w systemie zdalnie sterowanym (in Polish), Modelowanie inżynierskie, 31 (2017) 88–97.
27. Saków M., Parus A., Pajor M., Miądlicki K., Nonlinear inverse modeling with signal prediction in bilateral teleoperation with force-feedback, Methods and Models in Automation and Robotics (MMAR), 2017 22nd International Conference on, /IEEE, 2017, pp. 141–146.
28. Seraji H., Colbaugh R., Adaptive force-based impedance control, Intelligent Robots and Systems '93, IROS '93. Proceedings of the 1993 IEEE/RSJ International Conference on, 1993, pp. 1537–1544 vol. 1533.
29. Seul J., Hsia T.C., Bonitz R.G., Force tracking impedance control of robot manipulators under unknown environment, IEEE Transactions on Control Systems Technology, 12 (2004) 474–483.
30. Stuart K.D., Majewski M., Intelligent Opinion Mining and Sentiment Analysis Using Artificial Neural Networks, International Conference on Neural Information Processing, Springer, 2015, pp. 103–110.
31. Stuart K.D., Majewski M., Trelis A.B., Intelligent semantic-based system for corpus analysis through hybrid probabilistic neural networks, International Symposium on Neural Networks, Springer, 2011, pp. 83–92.
32. Tadano K., Kawashima K., Development of 4-DOFs forceps with force sensing using pneumatic servo system, Proceedings 2006 IEEE International Conference on Robotics and Automation, 2006. ICRA 2006., 2006, pp. 2250–2255.
33. Taghizadeh M., Ghaffari A., Najafi F., Improving dynamic performances of PWM-driven servo-pneumatic systems via a novel pneumatic circuit, ISA Trans, 48 (2009) 512–518.
34. Takigami T., Oshima K., Hayakawa Y., Ito M., Application of self-sensing actuator to control of a soft-handling gripper, Control Applications, 1998. Proceedings of the 1998 IEEE International Conference on, 1998, pp. 902–906 vol. 902.
35. Wei Tech A., Khosla P.K., Riviere C.N., Feedforward Controller With Inverse Rate-Dependent Model for Piezoelectric Actuators in Trajectory-Tracking Applications, Mechatronics, IEEE/ASME Transactions on, 12 (2007) 134–142.
36. Yokokohji Y., Yoshikawa T., Bilateral control of master-slave manipulators for ideal kinesthetic coupling-formulation and experiment, Robotics and Automation, IEEE Transactions on, 10 (1994) 605–620.
37. Yong Z., Barth E.J., Impedance Control of a Pneumatic Actuator for Contact Tasks, Proceedings of the 2005 IEEE International Conference on Robotics and Automation, 2005, pp. 987–992.
38. Yuguo C., Self-Sensing Compounding Control of Piezoceramic Micro-Motion Worktable Based on Integrator, Intelligent Control and Automation, 2006. WCICA 2006. The Sixth World Congress on, 2006, pp. 5209–5213.
39. Zhang T., Jiang L., Wu X., Feng W., Zhou D., Liu H., Fingertip Three-Axis Tactile Sensor for Multifingered Grasping, Mechatronics, IEEE/ASME Transactions on, PP (2014) 1–11.
40. Zhou M., Ben-Tzvi P., RML Glove – An Exoskeleton Glove Mechanism With Haptics Feedback, Mechatronics, IEEE/ASME Transactions on, 20 (2015) 641–652.